

# Supplemental Material for

## Origins and evolution of two types of Late Triassic granitic magmas in the Caolong-Xiangkariwa area of central-eastern Songpan-Ganze terrane, northern Tibet: Implications for pegmatite lithium mineralization

Jin-Heng Liu<sup>1,2,3,4</sup>, Qiang Wang<sup>1,2,3\*</sup>, Wu-Fu Li<sup>5</sup>, Bing-Zhang Wang<sup>5</sup>, Derek A. Wyman<sup>6</sup>, Lin Ding<sup>7</sup>,  
He Wang<sup>3,4</sup>, Chuan-Bing Xu<sup>1,2,3</sup>, Shan-Ping Li<sup>5</sup>, Chun-Tao Wang<sup>5</sup>, Jian-Dong Liu<sup>5</sup>, Rong-Qing Zhang<sup>8</sup>,  
Zi-Long Wang<sup>1,2,3</sup>, Tong-Yu Huang<sup>1,2,3</sup>, Xin-Yuan Zhang<sup>5</sup>

<sup>1</sup> *State Key Laboratory of Isotope Geochemistry, Guangzhou Institute of Geochemistry, Chinese Academy of Sciences, Guangzhou 510640, China*

<sup>2</sup> *College of Earth and Planetary Sciences, University of Chinese Academy of Sciences, Beijing 100049, China*

<sup>3</sup> *CAS Center for Excellence in Deep Earth Science, Guangzhou, 510640, China*

<sup>4</sup> *CAS Key Laboratory of Mineralogy and Metallogeny, Guangzhou Institute of Geochemistry, Chinese Academy of Sciences, Guangzhou 510640, China*

<sup>5</sup> *Qinghai Geological Survey Institute, Xining 810012, Qinghai, China*

<sup>6</sup> *School of Geosciences, The University of Sydney, Sydney, NSW 2006, Australia*

<sup>7</sup> *Institute of Tibetan Plateau Research, Chinese Academy of Sciences, Beijing, China*

<sup>8</sup> *State Key Laboratory for Mineral Deposits Research, School of Earth Sciences and Engineering, Nanjing University, Xianlin University Town, 210023 Nanjing, China*

E-mail address: [wqiang@gig.ac.cn](mailto:wqiang@gig.ac.cn) (Q. Wang)

## **Contents of this file**

### **1. Analytical methods**

1.1 Dating methods and SIMS O isotope

1.2 whole rock major-trace element composition and Sr-Nd isotope analyses

1.3 Major element and *in-situ* trace analyses of K-feldspar and mica

### **2. Supplementary figures (S1 to S5)**

Fig. S1 Field photographs of the TZX intrusive rocks, Caolong granites and pegmatites, and (meta)sedimentary rocks

Fig. S2 Photomicrographs of selected diorites, granodiorites, granites, and pegmatites from the TZX and Caolong samples

Fig. S3 Chondrite-normalized REE patterns and primitive mantle-normalized trace element for the TZX intrusive rocks and Caolong granites

Fig. S4 Hark diagrams for the TZX intrusive rocks and Caolong granites.

Fig. S5 (A) Ba/La vs. Th/Yb and (B) La/Sm vs. Ba/Th for the TZX intrusive rocks; (C)  $\epsilon_{\text{Nd}}(t)$  vs.  $\text{SiO}_2$  (wt.%), (D)  $\epsilon_{\text{Nd}}(t)$  vs. Sr/Y, and (E)  $^{87}\text{Sr}/^{86}\text{Sr}$  vs.  $\text{SiO}_2$  (wt.%) for the TZX intrusive rocks, Caolong granites, and Caolong pegmatites

### **3. Supplementary references**

#### **Additional Supporting Information (Files uploaded separately)**

**Table S1** Dating and zircon O isotope data for the TZX diorite and granodiorite, Caolong granite, and Caolong pegmatite

**Table S2** Whole rock geochemical data for the TZX diorite and granodiorite, Caolong granite and pegmatite, and (meta)sedimentary rocks; Mass balance calculation and trace element modeling for the TZX diorite and granodiorite

**Table S3** Major-trace element data for the K-feldspar and muscovite from Caolong granite and pegmatite

## **1. Analytical methods**

### **1.1 Dating methods and SIMS O isotope**

#### ***Zircon U-Pb dating:***

All zircons were separated through magnetic separation and conventional heavy liquid techniques.

The zircon U-Pb dating analyses of samples 19ZD02-1 and 19XKRW03 were carried out at the State Key Laboratory of Isotope Geochemistry, Guangzhou Institute of Geochemistry, Chinese Academy of Sciences, Guangzhou, China (SKLaBIG-GIG-CAS). The isotope and trace compositions of zircon were analyzed by in-situ LA-ICP-MS with a spot size of 29  $\mu\text{m}$  (Resonetics RESolution S-155 laser + Agilent 7900). The helium gas that carries the ablated sample aerosol, is mixed with nitrogen and argon carrier gas as additional di-atomic gas to improve sensitivity, finally flows into ICP. Each analysis included back-ground acquisition with approximately 20-30 s and data acquisition with 50 s from the sample. The primary standard and secondary standard used to calibrate the U-Pb age of zircon is 91500 zircon and Plesovice zircon, respectively. The external calibration reference is reference material NIST 610, and Si is the internal standard to quantify elemental concentrations; In addition, the zircon U-Pb dating of samples 19ZD03-1, 20CD06-3, 20CD06-4, 20CD07-1, and 20CD09-2 was undertaken by LA-ICP-MS at the Guangzhou Tuoyan Analytical Technology Co., Ltd., Guangzhou, China. Laser sampling was performed using a NWR 193 laser ablation system. An iCAP RQ ICP-MS instrument was used to acquire ion-signal intensities. Argon was used as the make-up gas and mixed with the carrier gas via a Y-connector before entering the ICP. The spot size and frequency of the laser were set to 30  $\mu\text{m}$  and 6 Hz, respectively, in this study. The energy was 3.5 J/cm<sup>2</sup>. The standard reference materials are same with the materials used in the SKLaBIG-GIG-CAS. Finally, we use the

ICPMSDataCal to perform the data results (Lin et al., 2016; Liu et al., 2008).

### ***SIMS zircon O isotopes***

Zircon oxygen isotopic ratios of sample 19CL05-6 were tested in the identical composition zone or the dated domains of the U-Pb ablated position of the same zircon grains, which uses a CAMECA IMS-1280 ion microprobe at the SKLaBIG-GIG-CAS. During the measurement, a primary beam of  $^{133}\text{Cs}^+$  ions was accelerated at 10 kv and matched with a  $\sim 2$  nA energy intensity, and an electron flood gun was used for charge compensation. The more detailed analytical procedures were described by Li et al. (2013). The Penglai zircon standard ( $\delta^{18}\text{O}_{\text{VSMOW}} = 5.31\text{‰}$ ) was used to correct instrumental mass fractionation (Li et al., 2010). The internal precision of a single analysis was usually better than 0.2‰ for the  $^{18}\text{O}/^{16}\text{O}$  ratio. And the weighted mean of  $\delta^{18}\text{O}$  yielded by the Penglai zircon standard and Qinghu zircon is within error of the data from the Li et al. (2013).

### ***Coltan U-Pb dating***

Coltan minerals U-Pb dating was conducted at the State Key Laboratory for Mineral Deposits Research in Nanjing University, Nanjing, China. The laser spot size was 43  $\mu\text{m}$ , repetition rate was 4 Hz, and energy density was  $\sim 4$  J/cm<sup>2</sup> during the analyses. The dwell times were 30 ms for  $^{207}\text{Pb}$ ; 15 ms for  $^{204}\text{Pb}$ ,  $^{206}\text{Pb}$ , and  $^{208}\text{Pb}$ ; 10 ms for  $^{232}\text{Th}$  and  $^{238}\text{U}$ ; and 6 ms for other elements. Each spot analysis was composed of approximately 20 s of background data acquisition, 50 s of sample data acquisition, and 20 s of ablation cell flushing. Each cycle of analysis contained two NIST610 standards, two Coltan 139 standards, and one GSE-1G and BCR-2G standard, and eight unknowns. The U-Pb isotope data was corrected by the coltan 139 standard (ID-TIMS age of  $506 \pm 2.3$  Ma; Romer and Lehmann, 1995). The more detailed analytical procedures were described by Che et al. (2015).

### ***Cassiterite U-Pb dating***

The LA-ICP-MS U-Pb isotopic analysis of cassiterite was undertaken at the State Key Laboratory for Mineral Deposits Research, Nanjing University, China. The instrumental system consists of a Thermo Fisher iCAP Qc ICP-MS, coupled with an ASI RESolution LR 193-nm ArF laser. About 99% of the material ablated was washed out in less than 1.5 s due to the two-volume laser ablation cell (155 × 105 mm). The cassiterite grains were analyzed by using spot sizes of 74 and 43  $\mu\text{m}$ , a laser energy density of 4 J/cm<sup>2</sup>, and a repetition rate of 6 Hz. Three U-Pb reference and validation materials used are as follows: Yankee (YK) cassiterite, from a quartz vein in the Mole granite, New England, eastern Australia (TIMS U-Pb age of  $246.48 \pm 0.51$  Ma; [Carr et al., 2020](#)); Cligga Head (CLGH) cassiterite, Cornwall, southwest England (TIMS U-Pb age of  $285.14 \pm 0.25$  Ma; [Tapster and Bright, 2020](#)); XHL cassiterite, from Xianghualing skarn Sn deposit, Southern Hunan Province, South China (~152-154 Ma). They were textured twice every 12 and 6 sample measurements, respectively. In addition, each spot analysis consisted of approximately 20s for a background acquisition, followed by sample data acquisition with 40s. Isotopes were measured in time resolved mode. For U-Pb analysis, dwell times for each mass scan were For U-Pb analysis, dwell times for each mass scan were 8 ms for <sup>204</sup>Pb, 15 ms for <sup>206</sup>Pb and <sup>208</sup>Pb, 20 ms for <sup>238</sup>U, <sup>232</sup>Th, and <sup>207</sup>Pb, 15 ms for <sup>206</sup>Pb and <sup>208</sup>Pb, 8 ms for <sup>204</sup>Pb. Raw data reduction was performed offline by the software Iolite 4. Data uncertainties for isotopic ratios in cassiterite samples are 1 $\sigma$  ([Li et al., 2016](#)). The software IsoplotR was employed to calculate U-Pb ages. The detailed analysis procedure had be presented in [Li et al. \(2016\)](#) and [Zhang et al. \(2017a, b\)](#). The details of the data reduction procedure based on references with variable common Pb contents are referred to [Chew et al. \(2014\)](#) and [Zhang et al. \(2022\)](#).

#### ***Muscovite <sup>40</sup>Ar/<sup>39</sup>Ar dating***

The muscovite samples were washed repeatedly in a centrifuge tube using acetone and deionized

water. Samples packed in aluminum foil were placed into quartz tubes, and the discs were then Cd-shielded and irradiated in a reactor for 21 h. The ZBH-25 biotite standard yielded a flat age spectrum with a plateau age of  $132.7 \pm 0.1$  Ma ( $1\sigma$ ) (Wang, 1983). The mean J-values calculated from the standards are listed in Appendix 2. The mean mass discrimination value was  $1.00012 (\pm 0.5\%)$  per Dalton relative to the atmospheric ratio of  $298.56 \pm 0.31$ . Correction factors for interfering Ar isotopes were derived from irradiated  $\text{CaF}_2$  and  $\text{K}_2\text{SO}_4$ , and were  $(^{39}\text{Ar}/^{37}\text{Ar})_{\text{Ca}} = 5.97 \times 10^{-4}$ ,  $(^{36}\text{Ar}/^{37}\text{Ar})_{\text{Ca}} = 1.99 \times 10^{-4}$ , and  $(^{40}\text{Ar}/^{39}\text{Ar})_{\text{K}} = 6.30 \times 10^{-3}$ .  $^{40}\text{Ar}/^{39}\text{Ar}$  laser stepwise heating experiments were conducted at the SKLaBIG-GIG-CAS.

The matrix grains were step-heated by a  $\text{CO}_2$  (IR,  $10.4 \mu\text{m}$ ) laser fired on the crystals for 60 seconds. The released gases were first cleaned up in a newly designed gas purification system to remove moisture and Other impurities (Bai et al., 2018; He et al., 2016). The gas was further purified for Ar isotope analysis with two SAES NP10 Zr–Al getters at room temperature and  $\sim 400^\circ\text{C}$ . An ARGUS VI multi-collector mass spectrometer (ThermoFisher) was used to measure Ar isotope ratios, operated in static mode at a constant resolution of  $\sim 200$ . Measurements were carried out in the multi-collection mode using four faradays to measure mass 40 to 37 and a 0-background compact discrete dynode ion counter to measure mass 36. The raw data were processed using ArArCALC software (version 2.4; Koppers, 2002), and the ages were calculated using the decay constants recommended by Renne et al. (2010). Age uncertainties include all sources of errors and were calculated following Renne et al. (2010).

## 1.2 whole rock major-trace element composition and Sr-Nd isotope analyses

Bulk rock major element, trace element composition and Sr-Nd isotope analyses were processed

at Wuhan SampleSolution Analytical Technology Co., Ltd., Wuhan, China. The sample pretreatment of whole rock major element analysis was made by melting method. The flux is a mixture of lithium tetraborate, lithium metaborate and lithium fluoride (45:10:5). Oxidant and release agent were ammonium nitrate and lithium bromide, respectively, following heating to 1050 °C for 15 min. Zsx Primus II wavelength dispersive X-ray fluorescence spectrometer (XRF) produced by RIGAKU, Japan was used for the analysis of major elements in the whole rock, The X-ray tube is a 4.0Kw end window Rh target. The operation conditions are voltage of 50 kV and current of 60 mA. The standard curve uses the rock standard sample GBW07101-14. The relative standard deviation is less than 2%.

Trace element analysis of whole rock was conducted on Agilent 7700e ICP-MS. The detailed sample-digesting process was described as follows: Sample powder (200 mesh) were placed in an oven at 105 °C for drying of 12 hours; (2) weighting 50 mg sample powder was placed in a Teflon bomb, following in which adding 1 ml HNO<sub>3</sub> and 1 ml HF; (3) Teflon bomb was putted in a stainless steel pressure jacket and heated to 190 °C in an oven for >24 hours; (4) After cooling, the opened Teflon bomb was placed on a hotplate with 140 °C and then evaporated to incipient dryness, subsequently adding 1 ml HNO<sub>3</sub> and was evaporated to dryness again; (5) 1 ml of HNO<sub>3</sub>, 1 ml of MQ water and 1 ml internal standard solution of 1ppm In were added, and the Teflon bomb was resealed and placed in the oven at 190 °C for >12 hours; (6) finally, the solution was diluted to 100 g by adding 2% HNO<sub>3</sub> in a polyethylene bottle.

Sr-Nd isotope analyses were performed on a Neptune Plus MC-ICP-MS (Thermo Fisher Scientific, Dreieich, Germany). Analyses of the NIST 987 standard solution yielded <sup>87</sup>Sr/<sup>86</sup>Sr ratio of 0.710242±14 (2SD, n=345, which is identical within error to their published values 0.710248±12 (Zhang and Hu, 2020). Analyses of the GSB 04-3258-2015 standard yielded <sup>143</sup>Nd /<sup>144</sup>Nd ratio of 0.512440±6 (2SD,



n=31), which is identical within error to their published values ( $0.512438 \pm 6$  (2SD) [Li et al., 2017](#)). In addition, the USGS reference materials BCR-2 (basalt) and RGM-2 (rhyolite) yielded results of  $0.705012 \pm 22$  (2SD, n=63) and  $0.704173 \pm 20$  (2SD, n=20) for  $^{87}\text{Sr}/^{86}\text{Sr}$ ,  $0.512641 \pm 11$  (2SD, n=82) and  $0.512804 \pm 12$  (2SD, n=80) for  $^{143}\text{Nd}/^{144}\text{Nd}$ , respectively, which is identical within error to their published values ([Li et al. 2012](#); [Zhang and Hu, 2020](#)).

### 1.3 Major element and *in-situ* trace analyses of K-feldspar and mica

Mineral major-element compositions were performed on the JXA-8100 electron microprobe (EMP) at the SKLaBIG-GIG-CAS. Operating condition of accelerating voltage of 15 kV, beam diameter of 20 nA and diameter of 1-2  $\mu\text{m}$  was used for K-feldspar, muscovite and garnet analyses. Analytical uncertainties were generally below 2%. Detailed analytical procedures were described by [Huang et al. \(2007\)](#).

An ELEMENT XR (Thermo Fisher Scientific) ICP-MS system linked with a 193-nm (ArF) Resonetics RESolution M-50 laser ablation system is used to perform the *in-situ* mineral trace-element compositions at the SKLaBIG. Laser condition was set as beam size of 33  $\mu\text{m}$ , energy density of  $\sim 4 \text{ J cm}^{-2}$ , and repetition rate of 6Hz. We used a smoothing device to smooth the sample signal. Each spot analysis comprised 20 s gas blank collection and 30 s sample signal detection. We used the Si measured with the EPMA as the internal standard element. Three USGS reference glasses BHVO-2G, GSD-1G and BCR-2G were used to construct the calibration line of each element. The oxide molecular yield, which is indicated by the  $^{238}\text{U}^{16}\text{O}/^{238}\text{U}$  ratio, was less than 0.3%. The data reduction strategy and detailed experiment procedure are described in [Zhang et al. \(2018\)](#).

## 2. Supplementary figures (S1 to S5)

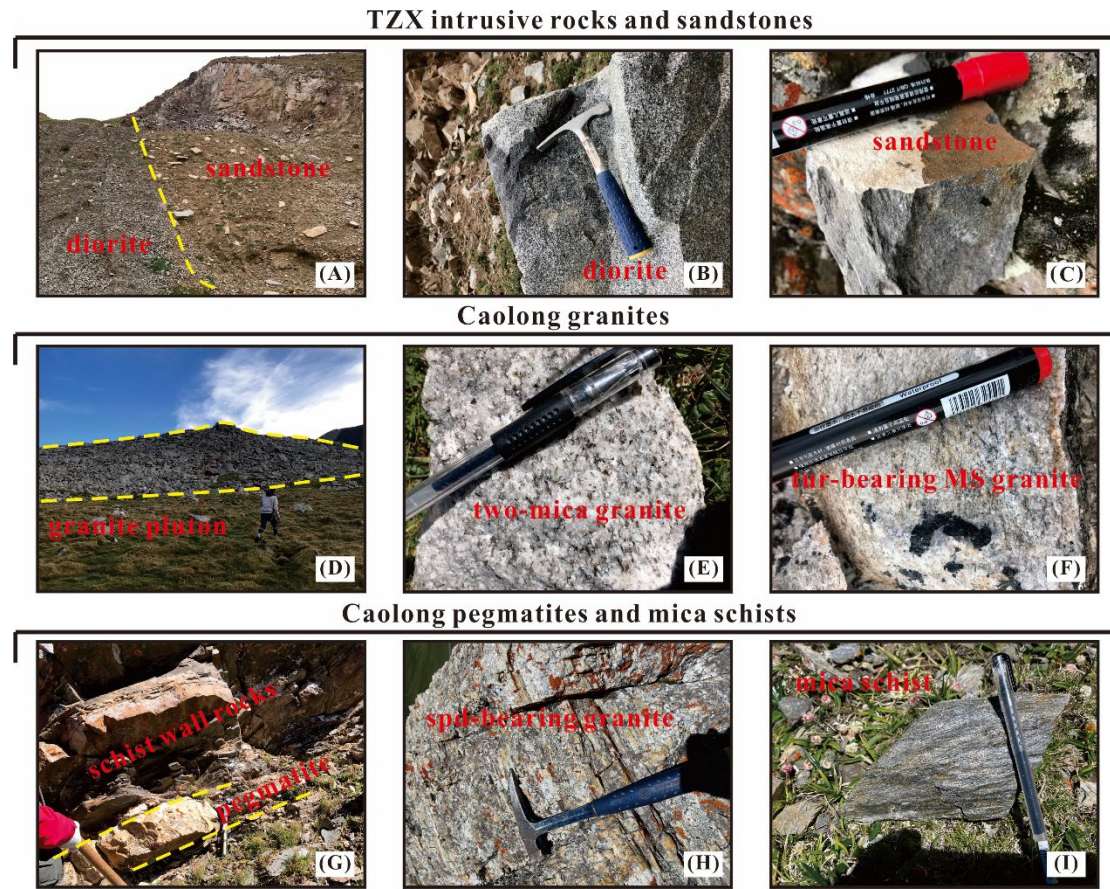


Fig. S1 (A–C) Field photographs of the TZX intrusive rocks and sandstone wall rocks; (D–f) Field photographs of the two-mica and muscovite granites from the Caolong pluton; (G–I) Field photographs of the pegmatites and schist wall rocks from the Caolong pluton.

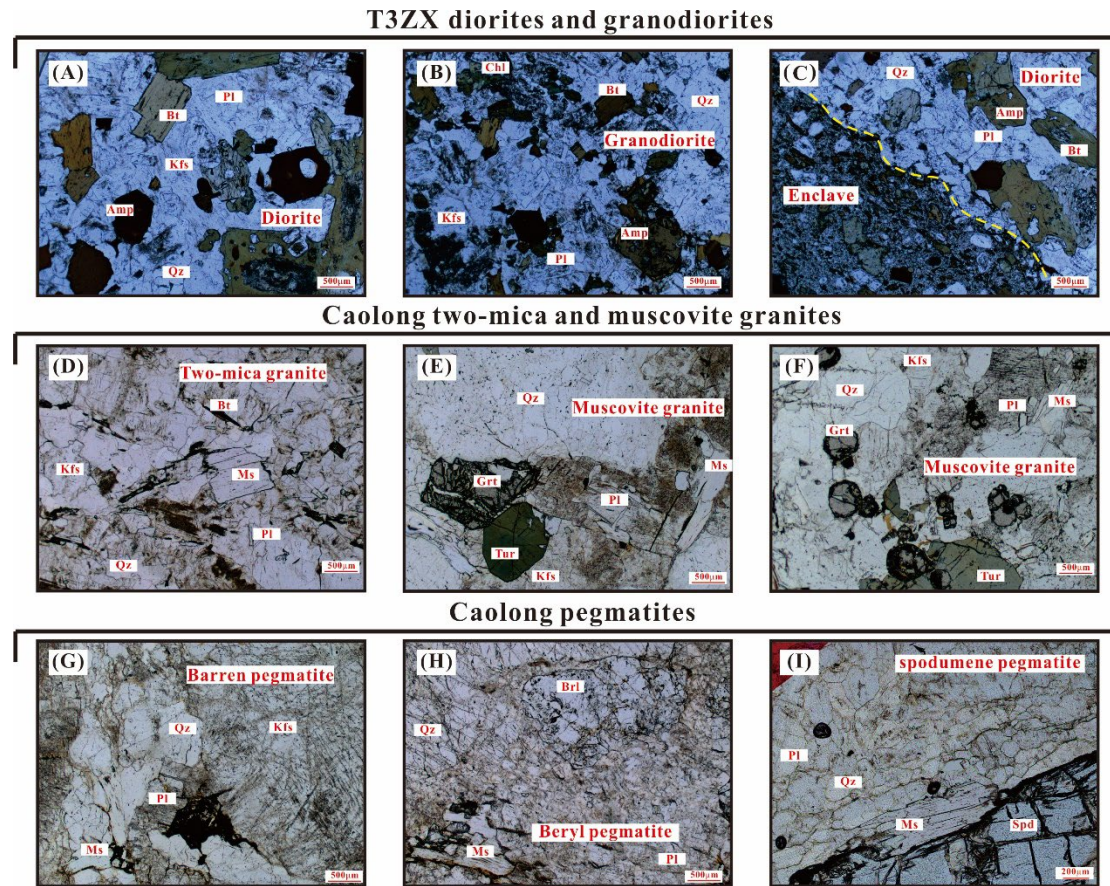


Fig. S2 Photomicrographs of selected diorites, granodiorites, granites, and pegmatites from the TZX and Caolong samples. (A–C) diorite, granodiorite, and enclave from the TZX plutons; (D–F) two-mica and muscovite granites from the Caolong pluton; (G–I) ore-barren pegmatite, beryl pegmatite, and spodumene pegmatites from the Caolong pluton.



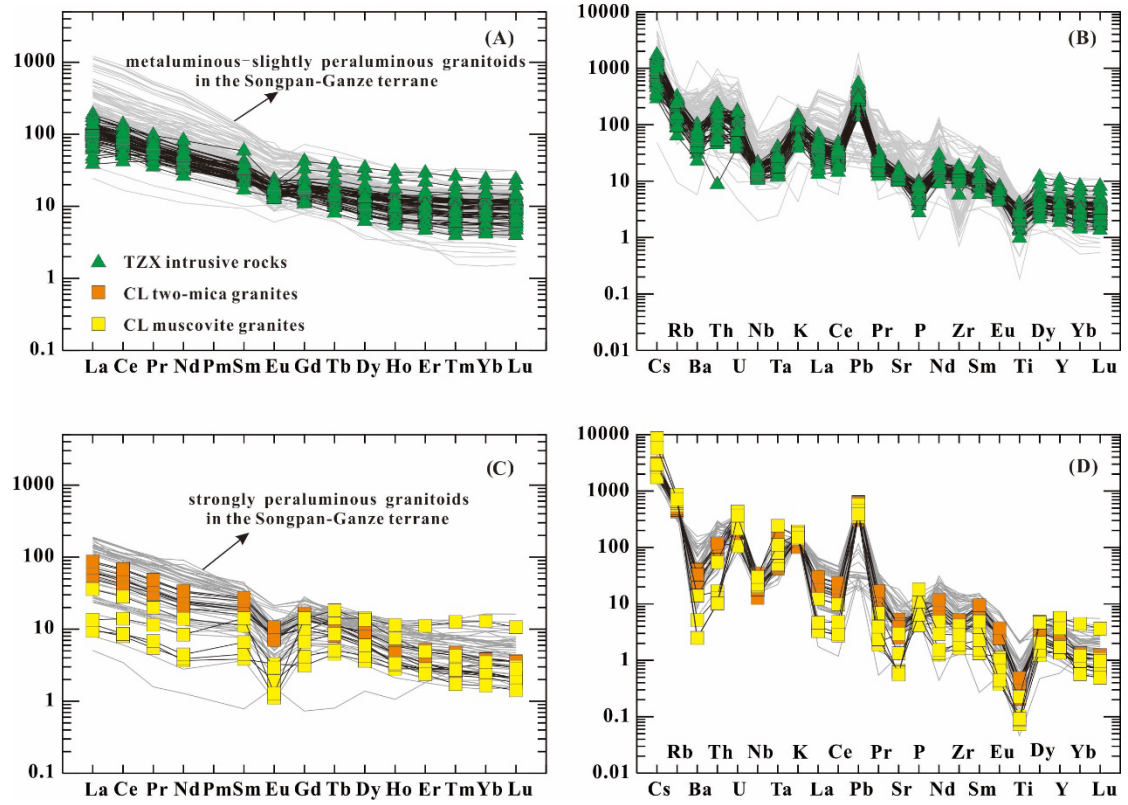


Fig. S3 (A and C) Chondrite-normalized REE patterns, and (C and D) Primitive mantle-normalized trace element for the TZX intrusive rocks and Caolong granites. Referenced data are as for Fig. 4.

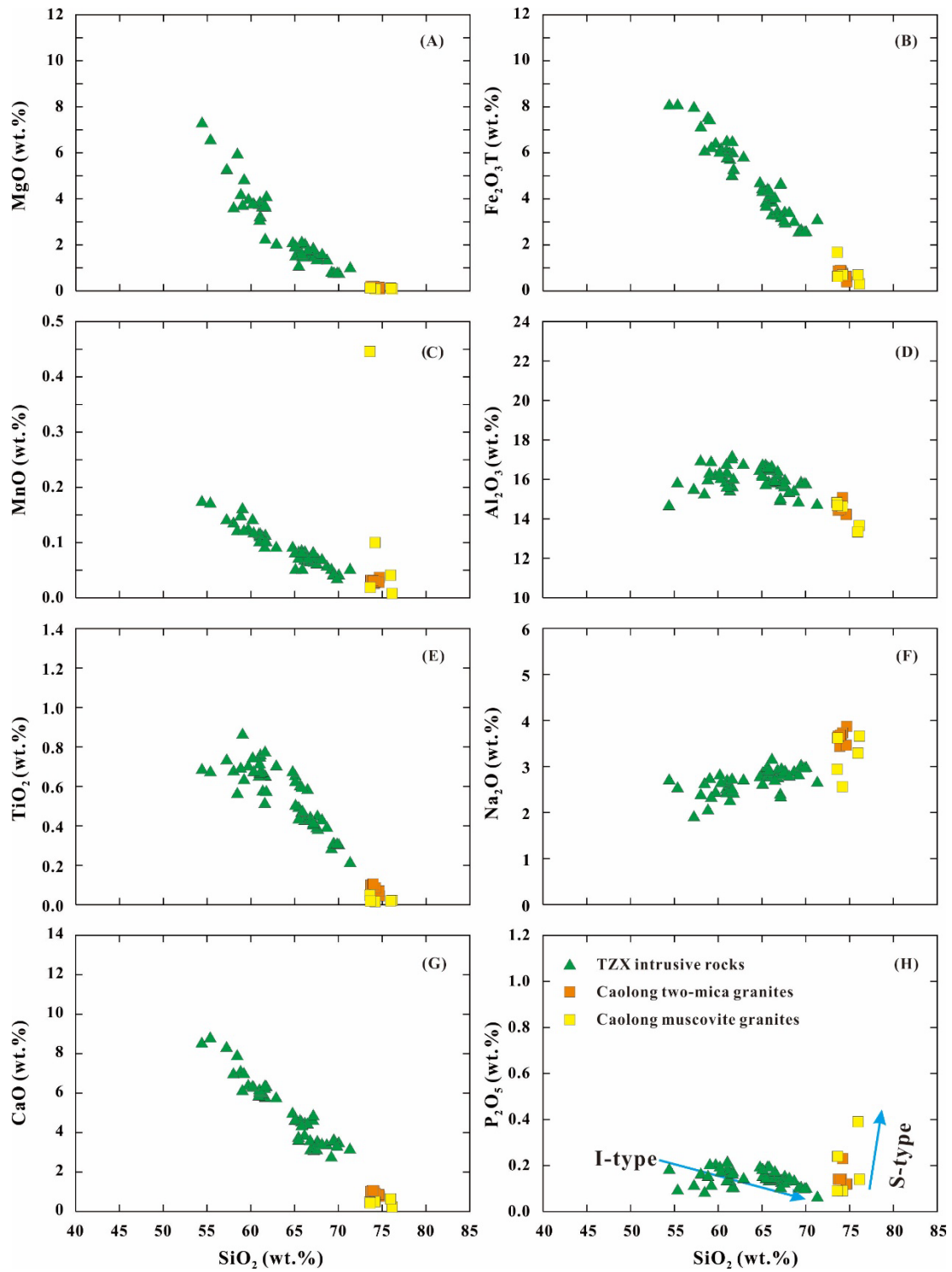


Fig. S4 Hark diagrams for the TZX intrusive rocks and Caolong granites.

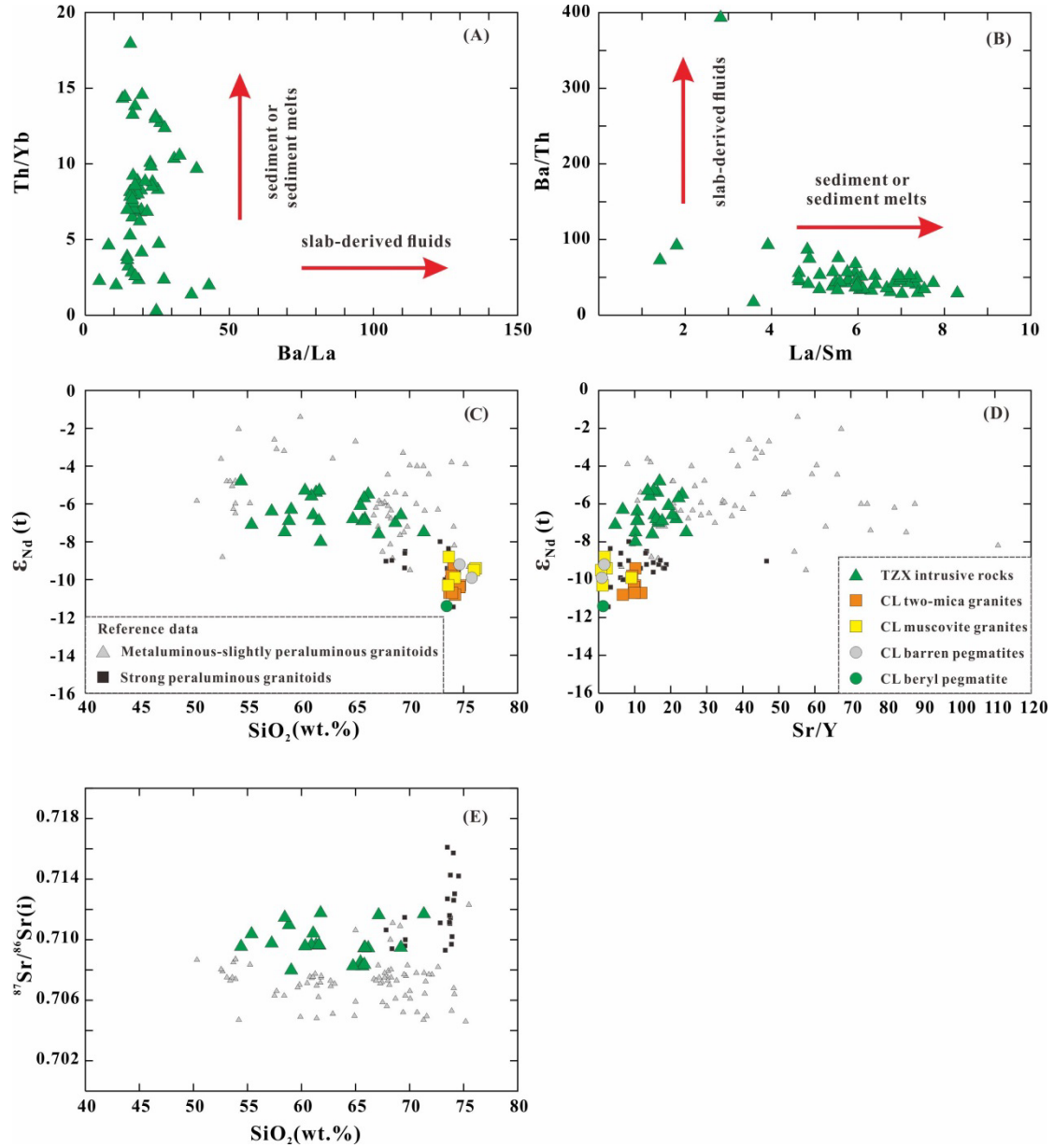


Fig. S5 (A) Ba/La vs. Th/Yb (Woodhead et al., 2001) and (B) La/Sm vs. Ba/Th (Labanich et al., 2012)

for the TZX intrusive rocks, suggesting that the metasomatized lithospheric mantle was formed by the addition of subduction sediment components; (C)  $\epsilon_{Nd}(t)$  vs.  $SiO_2$  (wt.%), (D)  $\epsilon_{Nd}(t)$  vs. Sr/Y, and (E)  $^{87}Sr/^{86}Sr$  vs.  $SiO_2$  (wt.%) for the TZX intrusive rocks, Caolong granites, and Caolong pegmatites, implying that the Caolong granites and pegmatite could not be generated by the evolution of TZX granitoids through fractional crystallization and crustal contamination. Symbols and referenced data are as for Fig. 4.

### 3. Reference

- Bai, X., Qiu, H., Liu, W. and Mei, L., 2018. Automatic  $^{40}\text{Ar}/^{39}\text{Ar}$  Dating Techniques Using Multicollector Argus Vi Noble Gas Mass Spectrometer with Self-Made Peripheral Apparatus: Journal of Asian Earth Sciences, v. 29(2), p. 408–415, <https://doi.org/10.1007/s12583-017-0948-9>.
- Carr, P.A., Zink, S., Bennett, V.C., Norman, M.D., Amelin, Y., Blevin, P.L., 2020. A new method for U-Pb geochronology of cassiterite by ID-TIMS applied to the Mole Granite polymetallic system, eastern Australia: Chemical Geology, v. 539, 119539, <https://doi.org/10.1016/j.chemgeo.2020.119539>.
- Che, X.D., Wu, F.Y., Wang, R.C., Gerdes, Axel., Ji, W.Q., Zhao, Z.H., Yang, J.H., Zhu, Z.Y., 2015. In situ U-Pb isotopic dating of columbite–tantalite by LA–ICP–MS: Ore Geology Reviews, v. 665, p. 978–989, <https://doi.org/10.1016/j.oregeorev.2014.07.008>.
- Chew, D.M., Petrus, J.A., Kamber, B.S., 2014. U-Pb LA-ICPMS dating using accessory mineral standards with variable common Pb: Chemical Geology, v. 363, p. 185–199, <https://doi.org/10.1016/j.chemgeo.2013.11.006>.
- He, L., Qiu, H. and Shi, H. et al., 2016. A Novel Purification Technique for Noble Gas Isotope Analyses of Authigenic Minerals: Science China Earth Sciences, v. 59(1), p. 111–117, <https://doi.org/10.1007/s11430-015-5159-6>.
- Huang, X.L., Xu, Y.G., Lo, C.H., Wang, R.C. Lin, C.Y., 2007. Exsolution lamellae in a clinopyroxene megacryst aggregate from Cenozoic basalt, Leizhou Peninsula, South China: petrography and chemical evolution: Contributions to Mineralogy and Petrology, v. 154, p. 691–705, <https://doi.org/10.1007/s00410-007-0218-4>.

- Koppers, A., 2002. Ararcalc-Software for  $^{40}\text{Ar}/^{39}\text{Ar}$  Age Calculations: Computers & Geosciences, v. 28(5), p. 605–619, [https://doi.org/10.1016/S0098-3004\(01\)00095-4](https://doi.org/10.1016/S0098-3004(01)00095-4).
- Li, C. F., Li, X. H., Li, Q. L., Guo, J. H., Yang, Y. H. (2012). Rapid and precise determination of sr and nd isotopic ratios in geological samples from the same filament loading by thermal ionization mass spectrometry employing a single-step separation scheme: Analytica Chimica Acta, v. 727(10), p. 54–60, <https://doi.org/10.1016/j.aca.2012.03.040>.
- Li, C.Y., Zhang, R.Q., Ding, X., Ling, M.X., Fan, W.M., Sun, W.D., 2016. Dating cassiterite using laser ablation ICP-MS: Ore Geology Reviews, v. 72, p. 313–322, <https://doi.org/10.1016/j.oregeorev.2015.07.016>.
- Li, X.H., Long, W.G., Li, Q.L., Liu, Y., Zheng, Y.F., Yang, Y.H., Chamberlain, K.R., Wan, D.F., Guo, C.H., Wang, X.C., 2010. Penglai Zircon Megacrysts: A Potential New Working Reference Material for Microbeam Determination of Hf–O Isotopes and U–Pb Age: Geostandards and Geoanalytical Research, v. 34, p. 117–134, <https://doi.org/10.1111/j.1751-908X.2010.00036.x>.
- Li, X.H., Tang, G.Q., Gong, B., Yang, Y.H., Hou, K.J., Hu, Z.C., Li, Q.L., Liu, Y., Li, W.X., 2013. Qinghu zircon: A working reference for microbeam analysis of U–Pb age and Hf and O isotopes: Chinese Science Bulletin, v. 58, p. 4647–4654, <https://doi.org/10.1007/s11434-013-5932-x>.
- Lin, J., Liu, Y.S., Yang, Y.H., Hu, Z.C., 2016. Calibration and correction of LA-ICP-MS and LA-MC-ICP-MS analyses for element contents and isotopic ratios. Solid Earth Sciences, v. 1(1), p. 5–27, <https://doi.org/10.1016/j.sesci.2016.04.002>.
- Liu, Y.S., Hu, Z.C., Gao, S., Gunther, D., Xu, J., Gao, C.G., Chen, H.H., 2008. In situ analysis of major and trace elements of anhydrous minerals by LA-ICP-MS without applying an internal standard: Chemical Geology, v. 257(1–2), p. 34–43, <https://doi.org/10.1016/j.chemgeo.2008.08.004>.



- Renne, P.R., Mundil, R., Balco, G., Min, K. and Ludwig, K.R., 2010. Joint Determination of  $^{40}\text{K}$  Decay Constants and  $^{40}\text{Ar}^*/^{40}\text{K}$  for the Fish Canyon Sanidine Standard, and Improved Accuracy for  $^{40}\text{Ar}/^{39}\text{Ar}$ : *Geochimica et Cosmochimica Acta*, v. 74(18), p. 5349–5367, <https://doi.org/10.1016/j.gca.2010.06.017>.
- Romer, R.L., Lehmann, B., 1995. U-Pb columbite–tantalite age of Neoproterozoic Ta–Nb mineralisation in Burundi: *Economic Geology*, v. 90, p. 2303–2309, <https://doi.org/10.2113/gsecongeo.90.8.2303>.
- Tapster, S., Bright, J.W., 2020. High-precision ID-TIMS cassiterite U–Pb systematics using a low-contamination hydrothermal decomposition: implications for LA-ICP-MS and ore deposit geochronology. *Geochronology*, v. 2, p. 425–441, <https://doi.org/10.5194/gchron-2-425-2020>.
- Wang, S., 1983. Age determinations of  $^{40}\text{Ar}/^{40}\text{K}$ ,  $^{40}\text{Ar}-^{39}\text{Ar}$  and radiogenic  $^{40}\text{Ar}$  released characteristics on K-Ar geostandards of china. Age determinations of  $^{40}\text{Ar}/^{40}\text{K}$ ,  $^{40}\text{Ar}-^{39}\text{Ar}$  and radiogenic  $^{40}\text{Ar}$  released characteristics on K-Ar geostandards of China: *Chinese Journal of Geology*, v. 18(4), p. 315–323.
- Zhang W., Hu Z.C. (2020). Estimation of isotopic reference values for pure materials and geological reference materials: *Atomic Spectroscopy*, v. 41(3), p. 93–102, <https://DOI:10.46770/AS.2020.03.001>.
- Zhang, L., Ren, Z.Y., Xia, X.P., Yang, Q., Hong, L.B., Wu, D., 2018. In situ determination of trace elements in melt inclusions using laser ablation-inductively coupled plasma-sector field-mass spectrometry: *Rapid Communications in Mass Spectrometry*, v. 33(4), p. 361–370, <https://doi.org/10.1002/rcm.8359>.
- Zhang, R.Q., Lehmann, B., Seltnann, R., Sun, W.D., Li, C.Y., 2017a. Cassiterite U-Pb geochronology

constrains magmatic-hydrothermal evolution in complex evolved granite systems: The classic Erzgebirge tin province (Saxony and Bohemia): *Geology*, v. 45, p. 1095–1098, <https://doi.org/10.1130/G39634.1>.

Zhang, R.Q., Lu, J.J., Hu, H., Gao, J.F., Zhou, M.Z., 2022. LA-ICPMS U-Pb dating of cassiterite using matrix-matched standards with variable common Pb: In preparation (a personal communication).

Zhang, R.Q., Lu, J.J., Lehmann, B., Li, C.Y., Li, G.L., Zhang, L.P., Guo, J., Sun, W.D., 2017b. Combined zircon and cassiterite U-Pb dating of the Piaotang granite-related tungsten-tin deposit, southern Jiangxi tungsten district, China: *Ore Geology Reviews*, v. 82, p. 268–284, <https://doi.org/10.1016/j.oregeorev.2016.10.039>.